Inorg. Chem. 1982, 21, 2987–2992

imental conditions as our Figure 4a and showed four redox couples in the potential range from +0.3 to −1.8 V vs. SCE. It was reported that every observed peak was due to a fully reversible one-electron transfer. Their first couple at $E_{1/2}$ = 0.02 V is about eight times smaller than that observed for the last three waves ($E_{1/2}$ = −0.74 V, $E_{1/2}$ = −1.14, and $E_{1/2}$ = −1.49 V), which are approximately equal. The couple at −0.74 V has been assigned as due to the reaction Mo^{V}/Mo^{IV} while that at more negative potentials as due to reduction at the porphyrin ring. The first reduction at ~0.02 V was assigned as due to reaction of $(TPP)Mo(O)(ClO_4)$ which is formed from a substitution of OCH_3^- by ClO_4^-, which is present as supporting electrolyte. Substitution of the methoxo group in $(TPP)Mo(O)(OCH_3)$ by acetate or chloride ion also resulted in this same effect,[11] i.e., an anodic shift (about 0.7 V) from that of the original peak at −0.71 V. However, these results with OAc^- or Cl^- are suspect due to the large concentration of common ion added to solution.

When the reported potentials for $(TPP)Mo(O)(OCH_3)$ reduction are considered, the results of Matsuda et al.[11] are, in part, consistent with our results. However, two fundamental differences are found in the actual cyclic voltammetric data. The first is that we observed, not four, but five redox couples in the potential range +0.3 to −1.8 V vs. SCE (Figure 4a). The second difference is that their couple at −0.76 V appears to be reversible while ours at −0.86 V is partially irreversible. No explanation is available as to the difference between the two studies, and, despite repeated attempts, we were unable to reproduce their data under the same experimental conditions. However, at low concentrations of supporting electrolyte (≤0.03 M), peaks III and IV are overlapped, yielding only a single process.

In summary, it is interesting to note that six-coordinate anionic forms of Mo^{IV} are formed in solution. Similar negatively charged ligated species have recently been reported in the form of $[(TPP)Fe^{II}]^-$[17] and $[(TPP)Mn^{II}X]^-$.[18] Of most interest is the nature of the ligand–metal bond in $(TPP)Mo(O)(OCH_3)$ and $[(TPP)Mo(O)OCH_3]^-$. From the existing data it appears that an equilibrium may exist between an ionic and a covalent form of the complex for both Mo^{V} and Mo^{IV}. Finally, these investigations have provided a necessary baseline for electrochemical studies which can be performed after dioxygen is reacted homogeneously with complexes of either $(TPP)Mo(O)$ or $(TPP)Mo(O)(OCH_3)$. This will be the basis of a later publication.

Acknowledgment. We gratefully acknowledge the National Science Foundation (Grant CHE-7921536) for support of this research.

Registry No. $(TPP)Mo(O)(OCH_3)$, 74751-79-4; $(TPP)Mo(O)$, 33519-60-7.

---

(17) Bottomley, L. A.; Kadish, K. M. *Inorg. Chem.* **1981**, *20*, 1348.
(18) Kadish, K. M.; Kelly, S. *Inorg. Chem.* **1979**, *18*, 2968.

Contribution from the Department of Chemistry,
University of Houston, Houston, Texas 77004

Electrochemical Characterization of a Novel Rhodium(II) Dimer, $Rh_2(ONHCCF_3)_4$

KARL M. KADISH,* D. LANÇON, A. M. DENNIS, and J. L. BEAR*

Received December 18, 1981

The electrochemical reactivity of a novel rhodium(II) dimer, $Rh_2(ONHCCF_3)_4$, was investigated in nonaqueous media. In all solvents investigated a one-electron oxidation was observed at potentials between +0.91 and +1.08 V vs. SCE. In seven solvents investigated this oxidation was reversible, but in pyridine or acetonitrile/pyridine mixtures a rapid chemical reaction followed the reversible oxidation. In THF an ill-defined irreversible reduction was also observed at −1.8 V vs. SCE. No other reduction or oxidation peak was observed in any of the solvents between +1.5 and −1.6 V. Measurements of pyridine binding were made by using both spectrophotometric and electrochemical techniques. In acetonitrile only a single pyridine ligand was observed to add to the complex. The stability constant for this ligand addition was 250. Finally, correlations were made between the electrochemical reactivity of the investigated complex and the nature of the solvent as well as comparisons to reactions of the similar rhodium(II) carboxylates, $Rh_2(O_2CCR)_4$.

Introduction

During recent years the electrochemistry and chemical reactivity of dinuclear rhodium(II) complexes have received considerable attention in the literature.[1-13] Investigations have included studies of both the kinetics and the thermodynamics of axial and equatorial ligand addition as well as studies of redox reactions to yield stable dimeric complexes of unusual oxidation states. Our own interest has been in the properties of rhodium(II) carboxylate dimers of the type $Rh_2(O_2CR)_4$ (shown in Figure 1a), where R varied from an electron-donating to an electron-withdrawing substituent.[14-18]

---

(1) Koh, Y. B.; Christoph, G. G. *Inorg. Chem.* **1978**, *17*, 2590.
(2) Christoph, G. G.; Koh, Y. B. *J. Am. Chem. Soc.* **1979**, *191*, 1422.
(3) Koh, Y. B.; Christoph, G. G. *Inorg. Chem.* **1979**, *18*, 1122.
(4) Christoph, G. G.; Halpern, J.; Khare, G. P.; Koh, Y. B.; Romanowski, C. *Inorg. Chem.* **1981**, *20*, 3029.
(5) Cotton, F. A.; Felthouse, T. R. *Inorg. Chem.* **1980**, *19*, 320.
(6) Cotton, F. A.; Felthouse, T. R. *Inorg. Chem.* **1980**, *19*, 323.
(7) Cotton, F. A.; Felthouse, T. R. *Inorg. Chem.* **1980**, *19*, 2347.
(8) Cotton, F. A.; Felthouse, T. R. *Inorg. Chem.* **1981**, *20*, 600.
(9) Kitchens, J.; Bear, J. L. *J. Inorg. Nucl. Chem.* **1969**, *31*, 2415.
(10) Drago, R. S.; Tanner, S. P.; Richman, R.; Long, J. R. *J. Am. Chem. Soc.* **1979**, *101*, 3897.
(11) Drago, R. S.; Long, J. R.; Cosmano, R. *Inorg. Chem.* **1981**, *20*, 2920.
(12) Cotton, F. A.; Felthouse, T. R. *Inorg. Chem.* **1981**, *20*, 584.
(13) Dikareva, L. M.; Porai-Koshits, M. A.; Sadikov, G. G.; Baranovsku, I. B.; Tolubnichaya, M. A.; Shchelokov, R. N. *Russ. J. Inorg. Chem.* (*Engl. Transl.*) **1978**, *23*, 1044.
(14) Das, K.; Simmons, E. L.; Bear, J. L. *Inorg. Chem.* **1977**, *16*, 1268.
(15) Howard, R. A.; Spring, T. G.; Bear, J. L. *Cancer Res.* **1976**, *36*, 4402.
(16) Dennis, A. M.; Howard, R. A.; Bear, J. L.; Korp, J. D.; Bernal, I. *Inorg. Chim. Acta* **1979**, *37*, L561.
(17) Das, K.; Kadish, K.; Bear, J. L. *Inorg. Chem.* **1978**, *17*, 930.

0020-1669/82/1321-2987$01.25/0

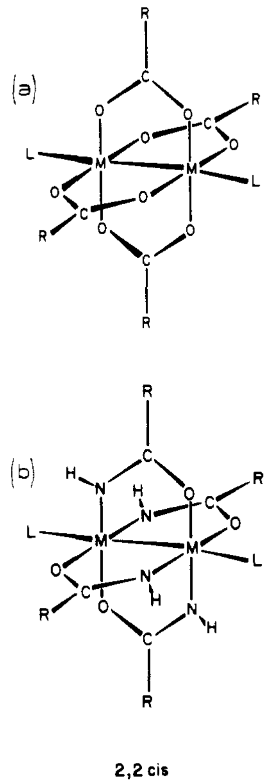

Figure 1. Structure of (a) $Rh_2(O_2CR)_4$ and (b) $Rh_2(ONHCCF_3)_4$.

In a recent publication we have reported on the electrochemistry of $Rh_2(O_2CR)_4$ in nonaqueous media.[17] Ten different complexes containing various R functions were investigated in nine different solvents. Independent of the solvent, the electrooxidation could always be characterized as a reversible one-electron abstraction to yield a Rh(2.5+) complex. This novel rhodium dimer has been characterized by ESCA,[18] electronic absorption spectroscopy,[19-21] and X-ray analysis[22] and could be reversibly reduced to yield the starting species. In contrast to the reversible oxidation process, reduction of the neutral $Rh_2(O_2CR)_4$ in both aqueous and nonaqueous media involved an initial irreversible one-electron transfer followed by a multielectron transfer step.[17] This reaction was not reversible and the products could not be isolated. These electrode reactions are shown as in eq 1. Half-wave potentials

$$[Rh_2(O_2CR)_4]^+ \underset{}{\overset{e^-}{\rightleftharpoons}} [Rh_2(O_2CR)_4] \xrightarrow{e^-} [Rh_2(O_2CR)_4]^- \xrightarrow{ne^-} \text{reduced products} \quad (1)$$

for both the oxidation and the reduction were characterized as a function of the solvent and the nature of the substituent, R.

In a preliminary communication we have reported the synthesis and physical characterization of a novel rhodium(II) dimer $Rh_2(ONHCCF_3)_4$.[23] The structure of this compound is shown in Figure 1b.[24] In this paper we wish to report, in detail, the electrochemical reactivity of this compound as a function of changes in solvent and axial ligand binding. Special emphasis is placed on the electron-transfer mechanisms in acetonitrile, pyridine, and acetonitrile/pyridine mixtures.

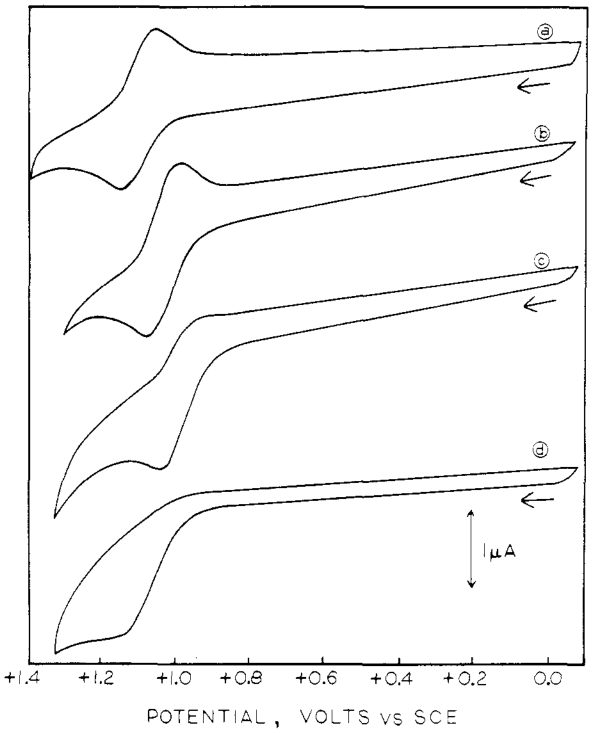

Figure 2. Cyclic voltammograms of 9.6×10^{-4} M $Rh_2(ONHCCF_3)_4$ in pyridine/acetonitrile mixtures at a scan rate of 0.05 V/s. The py:acetonitrile mole ratio is as follows: (a) 0:1; (b) 26:1; (c) 300:1; (d) 1:0.

Experimental Section

$Rh_2(ONHCCF_3)_4$ was synthesized by a reaction of CF_3CONH_2 and $Rh_2(O_2CCH_3)_4$ and then purified by high-performance liquid chromatography. The synthesis, purification, and physical properties of the complex are reported in a separate publication.[23]

The solvents nitromethane (CH_3NO_2), acetone (CH_3COCH_3), dimethylformamide (DMF), tetrahydrofuran (THF), acetonitrile (MeCN), *n*-butyronitrile (PrCN), benzonitrile (PhCN), dimethyl sulfoxide (Me_2SO), and pyridine were reagent grade quality. These were distilled from P_2O_5 and stored over 4-Å molecular sieves. For all experiments, the solvents contained 0.1 M tetrabutylammonium perchlorate (TBAP), as supporting electrolyte, which was recrystallized prior to use. All potentials were measured against those for dicyclopentadienyliron (ferrocene) in order to correct for liquid-junction potential differences between solvents. This compound was purchased from Aldrich Chemical Co. and used without further purification.

Polarographic measurements were made on Princeton Applied Research Models 173 and 174 electrochemical systems, utilizing a three-electrode geometry. The working electrode consisted of either a dropping mercury electrode (DME) or a platinum button electrode. A commercial calomel electrode was used as the reference electrode, and a platinum wire was used as the auxiliary electrode. The reference electrode was separated from the bulk of the solution by a bridge filled with solvent and supporting electrolyte; solutions in the bridge were changed periodically. Total volume utilized was 5–10 mL, and $Rh_2(ONHCCF_3)_4$ concentrations were between 10^{-3} and 10^{-4} M. Linear- and cyclic-sweep rates were varied between 0.05 and 0.5 V/s. The polarograms were recorded on a Princeton Applied Research Model 9002A XY recorder.

For controlled-potential coulometry, a Princeton Applied Research Model 173 potentiostat was used to control the potential at which experiments were run. Current–time curves were recorded on a PAR Model 9002A XY recorder. Integration of the current–time curve was achieved by means of a PAR Model 179 integrator. Large coiled platinum wires served as both the anode and cathode, which were separated by means of a fritted-glass disk. A commercial saturated calomel electrode was used as the reference electrode. Deaeration and stirring were achieved by means of a stream of high-purity nitrogen, which was passed throughout the solution. All potentials are reported either with respect to the saturated calomel electrode

---

(18) Dennis, A. M.; Howard, R. A.; Kadish, K. M.; Bear, J. L.; Brace, J.; Winograd, N. *Inorg. Chim. Acta* **1980**, L139.

(19) Wilson, C. R.; Taube, H. *Inorg. Chem.* **1975**, *14*, 2276.

(20) Wilson, C. R.; Taube, H. *Inorg. Chem.* **1975**, *14*, 205.

(21) Cannon, R. D.; Powell, D. B.; Saraurels, K.; Stillman, J. S. *J. Chem. Soc., Chem. Commun.* **1976**, *31*.

(22) Ziolkowski, J. J.; Moszner, M.; Glowiak, T. *J. Chem. Soc., Chem. Commun.* **1977**, *760*.

(23) Dennis, A. M.; Howard, R. A.; Lançon, D.; Kadish, K. M.; Bear, J. L. *J. Chem. Soc., Chem. Commun.* **1982**, 399.

(24) Dennis, A. M.; Korp, J. D.; Bear, J. L.; Bernal, I., paper on X-ray structure of $Rh_2(ONHCCF_3)_4(py)_2$ in preparation.

Table I. Half-Wave Potentials and Electrochemical Parameters for the Oxidation of $Rh_2(ONHCCF_3)_4$ in Nonaqueous Media

solvent	DN[a]	$E_p^a - E_{p/2}^a$, mV	$E_p^c - E_{p/2}^c$, mV	$E_p^a - E_p^c$, mV	$E_{1/2}$, V vs. SCE	$E_{1/2}$, V vs. Fc^+/Fc
$MeNO_2$	2.7	80	60	70	1.08	0.75
PhCN	11.1	70	85	65	1.13	0.66
MeCN	14.1	60	80	160	1.09	0.68
PrCN	16.6	60	60	135	1.07	0.61
Me_2CO	17.0	60	80	100	1.08	0.59
THF	20.0	65	60	220	1.15	0.57
DMF	26.6	70	60	100	0.91	0.43

[a] Reference 31.

(SCE) or with respect to the ferrocene/ferrocenium couple.

A Cary 14 spectrophotometer or a Tracor Northern 1710 holographic optical spectrometer/multichannel analyzer was used to obtain electronic absorption spectra. The Tracor Northern spectra result from the signal averaging of 100 sequential 5-ms spectral acquisitions; each of them represents a single spectrum from 325 to 950 nm, simultaneously recorded by a diode-array detector with a resolution of 1.2 nm/channel.

Results and Discussion

Figure 2a illustrates a typical cyclic voltammogram of $Rh_2(ONHCCF_3)_4$ in acetonitrile, 0.1 M TBAP. Only a single electron-transfer process was observed between +1.5 and −1.5 V vs. SCE. Similar cyclic voltammograms containing a single reversible oxidation wave were obtained in PrCN, PhCN, $MeNO_2$, Me_2CO, and DMF. In contrast the more strongly bonding solvent pyridine gave an oxidation of the rhodium dimer, which could be characterized as an irreversible process. A broad peak was obtained on the forward step and no peak, or a very broadened peak, on the backward sweep. Such a typical voltammogram can be seen in Figure 2d in neat pyridine and in Figure 2b,c in pyridine/acetonitrile mixtures. Finally, in THF, an irreversible reduction was also obtained at negative potentials, which was not observed in any other solvent. This reduction was not investigated in detail, and we have limited the scope of this paper to oxidations only.

Half-wave potentials were measured for the single oxidation process in seven different nonaqueous solvents and are listed in Table I. This table also includes the measured values of $E_p - E_{p/2}$, as well as the difference between the anodic and cathodic peak, $E_p^a - E_p^c$. Half-wave potentials vs. the saturated calomel electrode, as well as the more thermodynamic value of $E_{1/2}$ vs. the Fc^+/Fc couple, are presented.

The electrochemical oxidations in weakly bonding solvents are straightforward and uncomplicated. Diagnostic plots of $E_p - E_{p/2}$ and $E_p^a - E_p^c$ are in the range of that predicted for a one-electron transfer.[25] The peak current is proportional to the square root of scan rate and $i_{pa}/i_{pc} = 1$, indicating a diffusion-controlled one-electron transfer.[25] On the basis of these data the proposed electrode mechanism is eq 2. Assignment of bound solvent molecules is based on analogy to similar complexes of $Rh_2(O_2CCR)_4$, which are known to bind two solvent molecules in the oxidized and reduced forms.[26]

$$Rh_2(ONHCCF_3)_4(S)_2 \rightleftarrows [Rh_2(ONHCCF_3)_4(S)_2]^+ + e^- \tag{2}$$

Verification of the overall number of electrons transferred in reaction 2 was obtained when solutions of $Rh_2(ONHCCF_3)_4$ or $[Rh_2(ONHCCF_3)_4(S)_2]$ were oxidized at a controlled potential and the cyclic voltammograms recorded before and after total electrolysis. Values of *n* calculated for the oxidation and reduction of the complex are shown in Table II for MeCN and Me_2CO. Controlled-potential oxidations at potentials 200 mV more anodic than the half-wave potential showed an overall 1.0 electron was abstracted per dimeric unit (as the solution changed from pink to yellow in MeCN). This reaction was totally reversible as evidenced by the reversible cyclic voltammograms of the oxidation product as well as the fact that rereduction at a potential 200 mV more cathodic than the half-wave potential showed the addition of 1.0 electron/dimer and produced the original pink solution.

Table II. Coulometric Determination of the Number of Electrons Transformed/Mol of $Rh_2(ONHCCF_3)_4$[a]

solvent	oxidn	reredn
MeCN	0.97 ± 0.04	0.92 ± 0.02
Me_2CO	0.91 ± 0.05	0.85 ± 0.06

[a] Values presented are the average of five or more measurements.

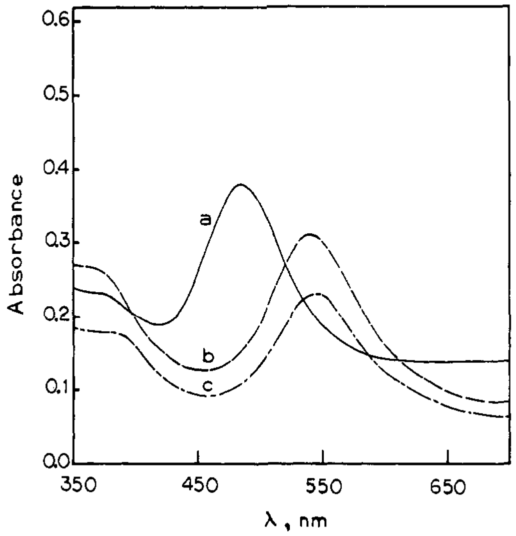

Figure 3. Electronic absorption spectra of $Rh_2(ONHCCF_3)_4$ in three solvents, with 0.1 M TBAP, at the following $Rh_2(ONHCCF_3)_4$ concentrations: (a) MeCN, 1.16×10^{-3} mol/L; (b) MeOH, 1.06×10^{-3} mol/L; (c) Me_2CO, 1.04×10^{-3} mol/L.

Electronic Absorption Spectra. Spectra taken during controlled-potential electrolysis at +1.30 V are shown in Figure 4, where the solvent is acetonitrile. The reduced form of $Rh_2(ONHCCF_3)_4$ (shown in Figure 3) is characterized by a band at 488 nm ($\epsilon_{max} = 260$) in MeCN, 546 nm in Me_2CO, and 538 nm in MeOH. In contrast, the oxidized form, $[Rh_2(ONHCCF_3)_4]^+$, has a strong band at 447–450 nm ($\epsilon_{max} = 3500$), which is virtually independent of solvent. This is shown in Figure 4 and was obtained by electrochemical oxidation in MeCN.

At this point it is appropriate to compare the visible spectra of the tetrakis(amidato)dirhodium complexes to the calculated and observed electronic transitions of the carboxylato-bridged rhodium species. Norman and co-workers[27,28] have assigned the two bands in the visible solution spectra of $Rh_2(O_2CR)_4L_2$ to allowed $\pi^* \rightarrow \sigma^*$ and $\pi^* \rightarrow$ Rh–O σ^* transitions. The assignment was based on the close match between calculated and experimental energies and the observed shifts in band energies with varying axial ligands, L. Single-crystal polarized spectra of $Rh_2(O_2CCH_3)_4(H_2O)_2$ strongly support this assignment.[29] Both bands are found to be primarily *xy* polarized as predicted by Norman's calculations. This description is not

---

[25] Nicholson, R. S.; Shain, I. *Anal. Chem.* **1964**, *36*, 706.

[26] Bottomley, L. A., private communication.

[27] Norman, J. G., Jr.; Kolari, H. J. *J. Am. Chem. Soc.* **1978**, *100*, 791.

[28] Norman, J. G., Jr.; Ronzoni, G. E.; Case, D. A. *J. Am. Chem. Soc.* **1979**, *101*, 5256.

[29] Martin, D. S., Jr.; Webb, T. R.; Robbins, G. A.; Fanwick, P. E. *Inorg. Chem.* **1979**, *18*, 475.

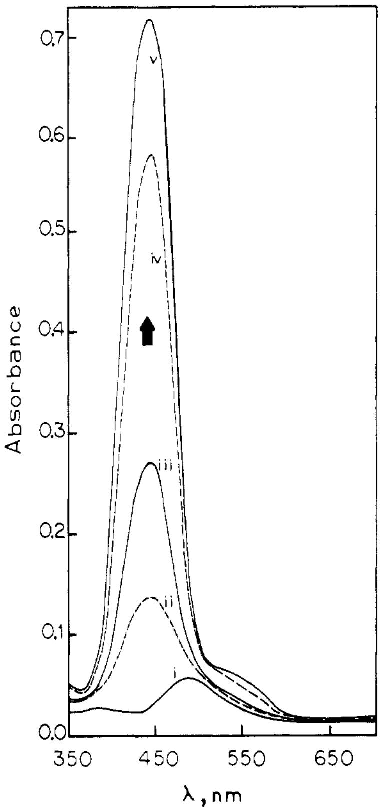

Figure 4. Electronic absorption spectra obtained during the oxidation of 9.5 × 10^{-4} M $Rh_2(ONHCCF_3)_4$ to yield $[Rh_2(ONHCCF_3)_4]^+$ in MeCN, with 0.1 M TBAP. $E_{applied}$ = +1.300 V/SCE. Total oxidation time per plot: (i) 0 s; (ii) 1 min 20 s; (iii) 2 min 30 s; (iv) 6 min; (v) 20 min.

true for all rhodium(II) carboxylate adducts. Recently, Bursten and Cotton have reported the results of Xα–SW molecular orbital calculations on the model compound $Rh_2(O_2CH)_4(PH_3)_2$.[30] Their results show that the σ interaction between the phosphine ligand and the $Rh_2(O_2CH)_4$ moiety is considerably stronger than the corresponding interaction with water. This results in a highest occupied molecular orbital of Rh–Rh σ and Rh–P σ* symmetry. The lowest energy transitions they predict for $Rh_2(O_2CH)_4(PH_3)_2$ are the Rh–Rh σ, Rh–P σ* → Rh–O σ* and the Rh–Rh σ, Rh–P σ* → Rh–Rh σ*, Rh–P σ transitions. It is well-known that the orbital pattern and resulting electronic transitions of the rhodium(II) carboxylates are strongly dependent on the binding characteristics of the axial ligand. A similar ligand dependency is observed for the tetraamidato-bridged dirhodium(II) adducts. Figure 3 shows the spectra of the amidato complex in methanol, acetone, and acetonitrile. The visible spectra in all three solutions show two bands. The lower energy band shifts to higher energy when the donor atom of the axial ligand is changed from oxygen to nitrogen. The higher energy band, a shoulder at ~370 nm, is fairly insensitive to the nature of the axial ligand. The behavior of the two transitions is quite similar to that observed for the carboxylato-bridged complexes. The basic difference in the visible spectra of the amidato- and carboxylato-bridged dimers with a given axial ligand is a ~40- and ~70-nm shift, in a hypsochromic direction relative to rhodium(II) acetate, for the low-energy and high-energy bands, respectively. Even though theoretical and experimental studies are needed, it is attractive to assign the low-energy band to the π* → σ* transition and the band at ~370 nm to some type of π* → Rh–O or Rh–N σ* transition. The solution spectrum of $[Rh_2(O_2CCH_3)_4(H_2O)_2]^+$ also contains two bands, but shifted to slightly higher energies than that observed for the neutral complex.[20] The qualitative difference between the visible spectra of the cation and neutral species is the appearance of a new low-energy band near 760 nm for $[Rh_2(O_2CCH_3)_4(H_2O)_2]^+$. Norman suggests that the band is due to either a δ → δ* transition or a O → δ* charge transfer. As seen in Figure 4, the spectrum for $[Rh_2(ONHCCF_3)_4]^+$ is very different from that of $[Rh_2(O_2CCH_3)_4]^+$. The oxidized amidato complex displays a strong band at 449 nm (ε = 3500) in MeCN and a weak band at 550 nm. The magnitude of the extinction coefficient of the band at 449 nm suggests it is due to a charge-transfer process. However, any attempt to assign the bands for $[Rh_2(ONHCCF_3)_4]^+$ at this time would be purely speculative.

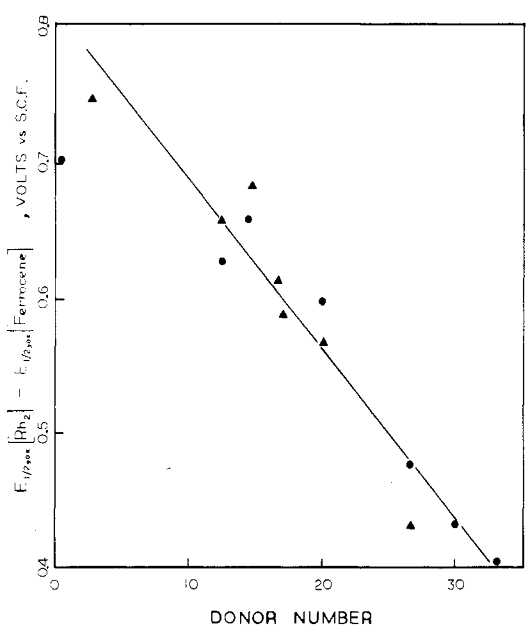

Figure 5. Half-wave potentials for oxidation of $Rh_2(ONHCCF_3)_4$ and $Rh_2(O_2CC_2H_5)_4$ vs. Gutmann donor number. The exact values of $E_{1/2}$ are given in Table I for the former compound (▲) and ref 17 for the latter compound (●).

Solvent Effects on Electrode Reactions. In order to systematize the effect of solvent on half-wave potentials, we constructed plots of $E_{1/2}$ vs. the solvent donor number. Seven solvents were utilized which varied from the weakly bonding nitromethane (DN = 2.7) to the strongly bonding DMF (DN = 26.6).[31] This relationship is shown in Figure 5. Also included in this figure are half-wave potentials taken from ref 17 for oxidation of $Rh_2(O_2CC_2H_5)_4$. The half-wave potentials for both series of complexes are plotted vs. that of the ferrocene/ferrocenium redox couple in order to eliminate the contributions due to liquid-junction potential.[32]

Generally, the higher oxidation state of an oxidation/reduction couple is stabilized relative to the lower oxidation state by solvent coordination, and the net effect is a cathodic shift of potential with increased donor number of the solvent.[31] This is observed for the complexes in this study and indicates a stronger solvent-binding ability of the (formally) mixed-oxidation-state dimer than of the neutral Rh(II) complex. It is extremely interesting to note from Figure 5 that an identical solvent effect (slope of $E_{1/2}$ vs. DN) is observed for both $Rh_2(O_2CC_2H_5)_4$ and $Rh_2(ONHCCF_3)_4$ and, in fact, potentials are almost superimposable between the two complexes. This latter fact is totally unexpected and can only be explained from

---

(30) Bursten, B. E.; Cotton, F. A. *Inorg. Chem.* **1981**, *20*, 3042.

(31) Gutmann, V. "The Donor-Acceptor Approach to Molecular Interactions"; Plenum Press: New York, 1978.

(32) Sawyer, D. T.; Roberts, J. C. "Experimental Electrochemistry for Chemists"; Wiley: New York, 1974.

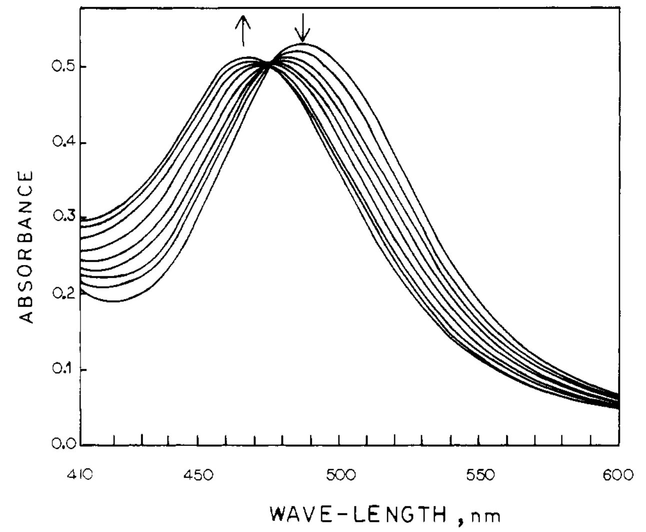

Figure 6. Electronic absorption spectra obtained during titration of 4.7×10^{-3} M $Rh_2(ONHCCF_3)_4$ with pyridine, into solutions of acetonitrile, with 0.1 M TBAP. The final pyridine concentration corresponds to 11 equiv.

a comparison of similar complexes of Rh(II) dimers containing CF_3 as a substituent.

Unfortunately, $Rh_2(O_2CCF_3)_4$ is extremely difficult to oxidize and no oxidation has been observed in the potential range of any solvent utilized. We can, however, estimate a value for its oxidation potential from the measured potentials of the remaining series of complexes, $Rh_2(O_2CR)_4$. In our prior electrochemical study of $Rh_2(O_2CR)_4$ we found that, in a given solvent, the potential difference between the first reduction and the first oxidation potential of all complexes was constant and independent of the nature of the R group.[17] This was true despite the fact that all oxidations were reversible and all reductions irreversible. For example, in DMF, plots of the oxidation vs. the reduction potentials taken from ref 17 are linear and the separation $E_{1/2}^{ox} - E_{1/2}^{red}$ is constant at 2.6 ± 0.1 V for all of the compounds investigated in this solvent. Thus, from the measured $E_{1/2} = -1.1$ V for reduction of the $Rh_2(O_2CCF_3)_4$ complex, a predicted oxidation step would occur at +1.6 V/SCE, which is beyond the potential limit of DMF. The $Rh_2(ONHCCF_3)_4$ complex investigated in this study has an oxidation at approximately +0.90 V in DMF. Therefore one can conclude that a change from oxygen to nitrogen as one of the bridging atoms stabilized the higher oxidation state of the complex by 700 mV. This difference corresponds to an increased stability of the higher oxidation state in $Rh_2(ONHCCF_3)_4$ by greater than 10^{10} with respect to $Rh_2(O_2CCF_3)_4$. (The greater the stabilization of the oxidized form, the easier the oxidation.) At the same time the substitution of a N atom for an O atom has shifted the reduction potential (to yield the Rh^{II}–Rh^{I} species) such that, in all but one solvent (THF), no evidence of reduction was observed. If one can assume that a similar value of $E_{1/2}^{ox} - E_{1/2}^{red} = 2.6$ V exists for $Rh_2(ONHCCF_3)_4$, a predicted value of $E_{1/2}^{red}$ would be ~ -1.7 V in DMF. A reduction was not observed in this solvent up to the potential limit at a platinum electrode of −1.8 V.

Electrode Reactions in Pyridine and Pyridine/Acetonitrile Mixtures. The number of pyridine molecules bound to the dimer in acetonitrile/pyridine mixtures was ascertained from monitoring both the change of potential as a function of pyridine concentration and changes in the electronic absorption spectrum. An example of the changes in spectra during a pyridine titration is shown in Figure 6. As py was added to acetonitrile solutions of $Rh_2(ONHCCF_3)_4$ a decrease in the absorption peak at $\lambda = 488$ nm occurred with a corresponding increase in the peak at $\lambda = 464$ nm. A single isosbestic point was observed at $\lambda = 475$ nm. Little change was observed in the molar absorptivities of the species.

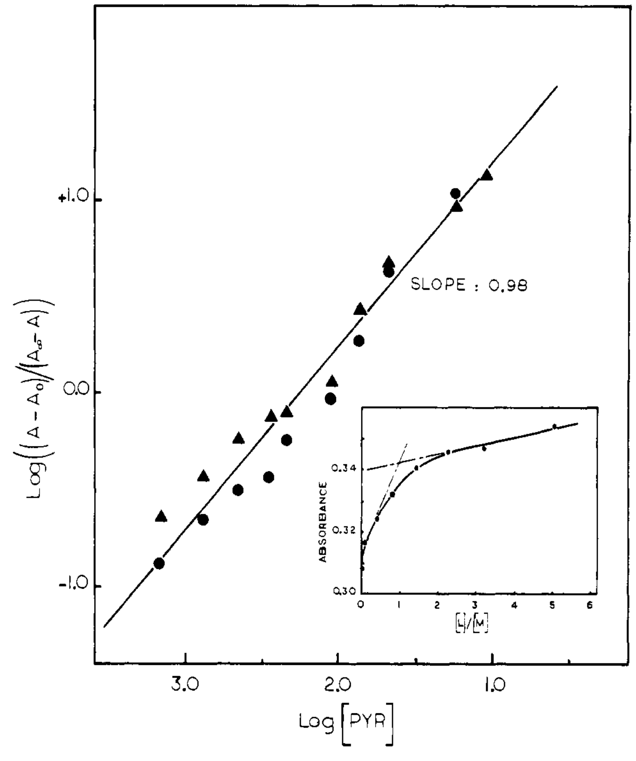

Figure 7. log–log plot and mole ratio obtained from data in Figure 6. Absorbances were measured at 464 (▲) and 488 nm (●).

Diagnostic plots of log $[(A - A_0)/(A_\infty - A)]$ vs. log [py] were constructed and are shown in Figure 7. Identical values were obtained at 488 and 464 nm and the slope was equal to 0.98, indicating the addition of only one pyridine ligand to the dimer in acetonitrile. This was true up to at least 500 equiv of pyridine. Conformation of a single ligand addition in this range of pyridine/acetonitrile mixtures was also obtained from the mole ratio plot (shown in the inset of Figure 7), where absorbance vs. the ratio of pyridine/Rh dimer gave a characteristic break in the plot for addition of a single pyridine molecule. On the basis of these data the addition of pyridine can be represented as in eq 3. Spectrophotometric determination of the equilibrium constant for reaction 3 using the data in Figure 7 gives a value of 2.5×10^2.

$$Rh_2(ONHCCF_3)_4(S)_2 + py \rightleftarrows Rh_2(ONHCCF_3)_4(S)(py) + S \quad (3)$$

Cyclic voltammograms of $Rh_2(ONHCCF_3)_4$ in pyridine and pyridine/acetonitrile mixtures have already been presented in Figure 2b–d. On the basis of the shape of the current–voltage curves, the lack of a reverse peak at high pyridine concentration, and the shift of E_p as a function of scan rate, the reaction can be assigned as consisting of an irreversible chemical reaction following a rapid electron transfer (an EC mechanism). Completely irreversible current–voltage curves were obtained when the mole ratio of pyridine to rhodium complex was greater than 500. At smaller concentrations of pyridine the rate of the chemical reaction following electron transfer was slower, and an ill-defined rereduction wave was obtained as shown in Figure 2b,c.

Plots of E_p^c and E_p^a vs. pyridine concentration were constructed at low pyridine concentration in order to determine the shift of potential upon complexation. From log [py] = −3.0 to −1.4, E_p^a shifted cathodically by 63 mV/log [py] while in the range of log [py] from −1.4 to 0, E_p^a was constant. This shift agrees with a theoretical displacement of 59 mV/log [py] if there was one more ligand on the oxidized form than on the reduced form of the complex.[33] On the basis of these data and the spectrophotometric results, the electrode reactions at low pyridine concentrations can correspond to reaction 4 while that at higher pyridine concentrations can correspond to reaction 5. As long as the initial reactant is not complexed by

$$Rh_2(ONHCCF_3)_4(S)_2 + py \overset{-e^-}{\rightleftharpoons} [Rh_2(ONHCCF_3)_4(py)(S)]^+ + S \quad (4)$$

$$Rh_2(ONHCCF_3)_4(py)(S) \overset{-e^-}{\rightleftharpoons} [Rh_2(ONHCCF_3)_4(py)(S)]^+ \quad (5)$$

pyridine the reaction remains reversible to quasi-reversible. However, at higher pyridine concentrations, pyridine will bind to the neutral complex and, in this case, the reaction begins to become irreversible. At very high pyridine concentrations the reaction is totally irreversible and, under these conditions, both the oxidized and the reduced forms of the complex may be bound by two pyridine molecules.

The exact cause of the irreversibility has not been identified. It is clear, however, that the lack of reverse peak is due to a chemical reaction that involves the oxidized species and that a similar reaction is observed for the oxidized rhodium(II) carboxylates in the presence of pyridine.[26] One explanation may be that the bridging ligands are partially dissociated with subsequent binding to the one or more vacant sites on the Rh_2^{4+} moiety by pyridine molecules. The new complex, whatever its stoichiometry, is electrochemically inactive in the range of potentials investigated. The complex is presently being investigated by other techniques.

In summary, we have shown in this study that electrochemical oxidation potentials for $Rh_2(ONHCCF_3)_4$ are similar to those of rhodium(II) acetate and propionate but surprisingly different from those of $Rh_2(O_2CCF_3)_4$. In our previous study of rhodium(II) carboxylates[17] it was observed that electron-withdrawing substituents help to stabilize the lower oxidation state of the metal. With a strong electron-withdrawing group like CF_3 the lower oxidation state is stabilized to such an extent that no oxidation step can be observed for $Rh_2(O_2CCF_3)_4$. The fact that $Rh_2(ONHCCF_3)_4$ is relatively easy to oxidize suggests that the substitution of nitrogen for oxygen in the bridging moiety results in a destabilization of the HOMO of the Rh–Rh bonding scheme approximately equal to the stabilization produced by the CF_3 substituent. Apparently the more basic nitrogen donor produces a greater electron density on the metal dimer than oxygen. This balancing of the two effects (change of atom in the ligand bridge and addition of an electron-withdrawing substituent) is not reflected in the reduction potentials. Contrary to the results of $Rh_2(O_2CCR)_4$ no reduction potentials are observed in any solvents except THF up to potentials of −1.9 V vs. SCE. This cathodic shift of $E_{1/2}$ suggests that the level of the LUMO is more sensitive than that of the HOMO to the change from $Rh_2(O_2CCF_3)_4$ to $Rh_2(ONHCCF_3)_4$ and that the difference between the HOMO and LUMO is greater in the latter complex than in the former. This observation qualitatively agrees with the observed spectral shift of the neutral complex toward shorter wavelengths. However, further detailed spectral and structural investigations are needed, which are presently under way.

Acknowledgment. Support of this research from the Robert A. Welch Foundation (K.M.K., Grant E-680; J.L.B., Grant E-196) is gratefully acknowledged.

Registry No. $Rh_2(ONHCCF_3)_4$, 81988-04-7.

---

[33] Crow, D. R. "Polarography of Metal Complexes"; Academic Press: London, 1969.

Contribution from Istituto di Chimica Analitica ed Elettrochimica,
University of Pisa, 56100 Pisa, Italy

Equilibria and Kinetics of Complex Formation at Gallium(III). Evidence for an Associative Mode of Activation

RICCARDO CORIGLI, FERNANDO SECCO,* and MARCELLA VENTURINI

Received June 18, 1981

The kinetics and equilibria of the reaction between gallium(III) and salicylic acid (H_2SAL), 5-chlorosalicylic acid (H_2ClSAL), 5-nitrosalicylic acid (H_2NSAL), and 3,5-dinitrosalicylic acid (H_2DNSAL) have been investigated in aqueous solution within an $[H^+]$ range between 0.0075 and 0.2 M at an ionic strength 0.2 M. Two complexes, GaL^+ and $GaHL^+$, were identified with H_2SAL, H_2ClSAL, and H_2NSAL whereas only GaL^+ was detected with H_2DNSAL. Complex formation constants and acid dissociation constants, K_{A1}, for the ligands (H_2L) have been evaluated by computer analysis of spectrophotometric data. The rate constants for reactions of Ga^{3+} with HL^- are linearly dependent of K_{A1} in a dilogarithmic plot as well as rate constants for reactions involving $Ga(OH)^{2+}$ and HL^-. The activation parameters have been determined in the case of H_2DNSAL. The evidences for an associative mechanism are discussed.

Introduction

Much of the current interpretation of the kinetic behavior of metal cations in labile octahedral complex formation is based on a proposal of Eigen[1] that the S_N1 ion-pair or "dissociative-interchange" mechanism is operative. The substantial literature that has accumulated rapidly since 1965, when Eigen and Wilkins' review[2] on this topic appeared, has confirmed this interpretation chiefly as regards bivalent metal cations[3-6] whereas the kinetic features of reactions of formation of labile complexes of tervalent cations are far less clear.[5-7]

In particular, little effort has so far been devoted to the reactions of gallium(III) ion.[8-13] This is probably due to

---

[1] Eigen, M. *Z. Elektrochem.* **1960**, *64*, 115. Eigen, M.; Tamm, K. *Ibid.* **1962**, *66*, 93, 107.

[2] Eigen, M.; Wilkins, R. G. *Adv. Chem. Ser.* **1965**, *No. 49*, 55.

[3] Langford, C. H.; Stengle, T. T. *Annu. Rev. Phys. Chem.* **1968**, *19*, 193.

[4] Hewkin, D. J.; Prince, R. H. *Coord. Chem. Rev.* **1970**, *5*, 45.

[5] Kustin, K.; Swinehart, J. "Inorganic Reaction Mechanisms"; Edwards, J. O., Ed.; Interscience: New York, 1970; p 107.

[6] *Inorg. React. Mech.* **1971-1977**, *1-5*.

[7] Perlmutter-Hayman, B.; Tapuhi, E. *Inorg. Chem.* **1979**, *18*, 875.

[8] Fiat, D.; Connick, R. E. *J. Am. Chem. Soc.* **1968**, *90*, 608.

[9] Miceli, J.; Stuehr, J. *J. Am. Chem. Soc.* **1968**, *90*, 6967.

[10] Kaway, Y.; Takahashi, T.; Hayashi, K.; Imamura, T.; Nakayama, H.; Funimoto, M. *Bull. Chem. Soc. Jpn.* **1972**, *45*, 1417.

0020-1669/82/1321-2992$01.25/0